Butadiene as a Ligand in Open Sandwich Compounds

Qunchao Fan, [a] Jia Fu,[a] Huidong Li,[a] Hao Feng,[a*] Weiguo Sun,[a]
Yaoming Xie,[b] R. Bruce King,[b*] and Henry F. Schaefer

[a]*School of Physics and Chemistry, Research Center for Advanced Computation, Xihua University, Chengdu, China 610039*
[b]*Department of Chemistry and Center for Computational Quantum Chemistry University of Georgia, Athens, Georgia 30602, USA*

rbking@chem.uga.edu; fenghao@mail.xhu.edu.cn

Abstract

Theoretical methods show that the lowest energy bis(butadiene)metal structures $(C_4H_6)_2M$ (M = Ti to Ni) have a perpendicular relative orientation of the two butadiene ligands corresponding to a tetrahedral coordination of the central metal atom to the four C=C double bonds of the butadiene ligands. Distribution of the metal d electrons in the resulting tetrahedral ligand field rationalizes the predicted spin states increasing monotonically from singlet to quartet from nickel to manganese and back from quartet to singlet from manganese to titanium.

1. Introduction

A major milestone in the development of transition metal organometallic chemistry was the serendipitous 1951 discovery of the sandwich compound ferrocene.[1,2] Shortly thereafter, analogous sandwich compounds, namely the metallocenes, were discovered for all of the other first row transition metals from vanadium to nickel (Figure 1). A key feature of such metallocenes is the presence of the cyclopentadienyl ligand. In fact, a common method of synthesizing metallocenes uses the reaction of the cyclopentadienide anion with metal halides.

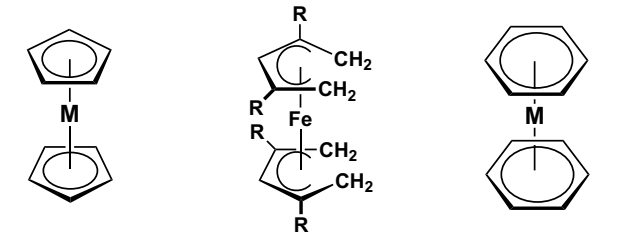

Figure 1. Examples of sandwich compounds.

Close relatives of the sandwich compounds are the so-called open sandwich compounds or open metallocenes containing an acyclic pentadienyl ligand. A wide range of such open sandwich compounds have been synthesized by Ernst and co-workers[3] by reactions of the acyclic pentadienide anion with metal halides (Figure 1). As might be expected, the open metallocenes were found to be less stable than the closed metallocenes. More stable open metallocenes were obtained by introducing alkyl substituents into the pentadienyl ligands.

Analogues of the metallocenes have been prepared with different ring sizes for the carbocyclic ligands. The most notable such derivatives include dibenzenechromium and related bis(arene) metal derivatives (Figure 1).[4] Introduction of cyclobutadiene ligands into sandwich compounds has proven to be more difficult because the instability of free cyclobutadiene restricts possible synthetic methods. However, indirect methods have been used to prepare cyclobutadiene metal complexes, most notably (cyclobutadiene)iron tricarbonyl, $(\eta^4\text{-}C_4H_4)Fe(CO)_3$ (Figure 2).[5] The only reported homoleptic bis(cyclobutadiene)metal sandwich compound is the nickel derivative $(\eta^4\text{-}Ph_4C_4)_2Ni$ but the proposed sandwich structure has not been verified structurally.[6,7]

The acyclic analogue of cyclobutadiene is the readily available and stable butadiene. It is therefore not surprising that the discovery of the first butadiene metal complex predates the seminal discovery of ferrocene by approximately two decades.

Thus in 1930 Reihlen and co-workers[8] found that the reaction of butadiene with iron pentacarbonyl in an autoclave gives butadiene iron carbonyl as a stable distillable liquid. However, the nature of butadiene iron tricarbonyl remained obscure until well after the initial discovery of ferrocene when Hallam and Pauson[9] reinvestigated its synthesis in 1958. A subsequent structure determination by Mills and Robinson[10] using X-ray crystallography at –40° confirmed the tetrahapto bonding of the butadiene ligand to the $Fe(CO)_3$ moiety (Figure 2).

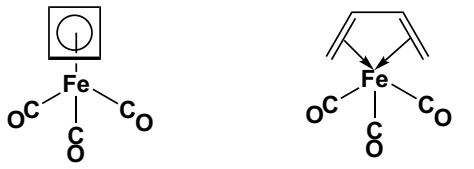

Cyclobutadiene iron tricarbonyl Butadiene iron tricarbonyl

Figure 2. Comparison of cyclobutadiene iron tricarbonyl and butadiene iron tricarbonyl.

Despite the discovery of butadieneiron tricarbonyl nearly 90 years ago, the chemistry of bis(butadiene)metal open sandwich complexes without additional ligands remains rather limited. In some cases cocondensation of metal atoms with butadiene or substituted butadienes provides a route to such complexes. Thus cocondensation of nickel atoms with butadiene at –78° gives an unstable volatile yellow liquid shown by mass spectrometry to have the formula $C_8H_{12}Ni$ and thus presumed to be bis(butadiene)nickel.[11] However, even though bis(butadiene)nickel has the favored 18-electron configuration this yellow liquid is reactive towards excess butadiene in the system thereby converting to a volatile red $C_{12}H_{18}Ni$ compound. The linear chain of 12 carbon atoms in this species is supported by the formation of n-dodecane upon hydrogenation. Thus $C_{12}H_{18}Ni$ is formulated as the bis(allylic) olefin complex ($\eta^{3,3,2}$-$C_{12}H_{18}$)Ni (Figure 3). This complex readily eliminates the nickel atom upon cyclization to 1,5,9-cyclododecatriene thereby making this 12-membered ring cyclic triolefin readily available from butadiene in large quantities.

The chemistry of zerovalent homoleptic $(butadiene)_2M$ derivatives is more extensive if the butadiene ligands are of the type RCH=CH–CH=CHR where R is a bulky substituent such as tert-butyl or trimethylsilyl. Thus cocondensation of metal vapors with 1,4-bis(tert-butyl)butadiene gives the corresponding $[C_4H_4(CMe_3)_2]_2M$ complexes (M = Ti,[12] V,[12] Co[13]). The cobalt derivative $[C_4H_4(CMe_3)_2]_2Co$ has a 17-electron configuration with the expected doublet ground state. It has been reduced to the monoanion $[\{C_4H_4(CMe_3)_2\}_2Co]^-$ having the favored 18-electron cobalt configuration.

This anion has been isolated as its potassium salt. Structural determination by X-ray crystallography indicates the expected bis(tetrahapto)butadiene metal open sandwich structure with the midpoints of the four C=C double bonds from the two butadiene ligands in an approximate tetrahedral coordination around the central cobalt atom. The zerovalent cobalt 1,4-bis(trimethylsilyl)butadiene derivative $[C_4H_4(SiMe_3)_2]_2Co$ has also been synthesized and structurally characterized.[14]

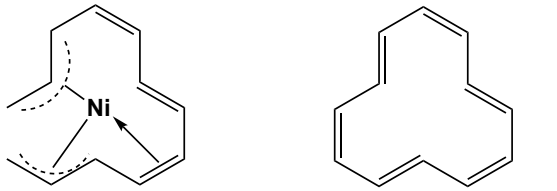

Figure 3. Structures of $(\eta^{3,3,2}\text{-}C_{12}H_{18})Ni$ obtained from nickel vapor and 1,3-butadiene and the butadiene trimer 1,5,9-cyclododecatriene.

The $(C_4H_6)_2M$ derivatives of the metal atoms to the left of nickel in the periodic table have less than the favored 18-electron metal configuration. Coordination with additional ligands can help the central metals attain or at least approach the favored 18-electron configuration. Thus a series of bis(butadiene)iron complexes of the type $(C_4H_6)_2FeL$ (L = CO,[15] PR_3[16]) are known in which the iron atom has the favored 18-electron configuration. Furthermore, bis(butadiene)manganese complexes of the type $(C_4H_6)_2MnL$ (L = CO,[17,18] PR_3[16,19]) provide extensive series of stable doublet spin state complexes in which the manganese atom has a 17-electron configuration.

This paper reports a theoretical study of the unsubstituted bis(butadiene)metal complexes of the first row transition metals, $(C_4H_6)_2M$. We find an approximately tetrahedral configuration of the four C=C double bonds in the two butadiene ligands to be energetically preferred in most systems. Thus the preferred spin states of the $(C_4H_6)_2M$ complexes can be rationalized on the basis of strong tetrahedral ligand field metal complexes.

2. Theoretical Methods

Electron correlation effects have been included by using density functional theory (DFT) methods, which have evolved as a practical and effective computational tool, especially for organometallic compounds.[20,21,22,23,24,25,26] The reliability of such density functional theory (DFT) methods is affected by the quality of the approximate exchange-

correlation (XC) energy functional. Initially two DFT methods (B3LYP and the BP86) were used. The B3LYP method is a hybrid HF/DFT method,[27,28] and the BP86 method combines Becke's 1988 exchange functional with Perdew's 1986 gradient-corrected correlation functional method.[29,30] However, Reiher and coworkers have found that B3LYP favors high-spin states and BP86 favors low-spin states.[31] This is also true in the present research so that these two DFT methods may predict global minima of different spin states. For this reason, Reiher and coworkers proposed a new parametrization for the B3LYP functional, named B3LYP*, which generally provides electronic spin state orderings in agreement with experiment.[32] In the present study, we will discuss the B3LYP* results in the text, while the results from other two methods are reported in the Supporting Information.

Double-ζ plus polarization (DZP) basis sets were used. For carbon atoms one set of spherical harmonic d functions with the exponent $\alpha_d(C) = 0.75$ was added to the standard Huzinaga-Dunning contracted DZ sets. This basis set is designated (9s5p1d/4s2p1d).[33,34] For hydrogen, a set of p polarization functions $\alpha_p(H) = 0.75$ was added to the Huzinaga-Dunning DZ sets. For the first row transition metals, in our loosely contracted DZP basis sets the Wachters primitive sets were used, but augmented by two sets of p functions and one set of d functions, contracted following Hood et al., and designated (14s11p6d/10s8p3d).[35,36]

The present paper discusses systems of the type $(C_4H_6)_2M$, where M is a first row transition metal from titanium to nickel. Thus the $(C_4H_6)_2M$ (M = Ti, Cr, Fe, Ni) structures were optimized for the singlet, triplet, and quintet electronic states, while the $(C_4H_6)_2M$ (M = V, Mn, Co) structures were optimized in the doublet, quartet, and sextet electronic states. The harmonic vibrational frequencies and the corresponding infrared intensities were determined at the same levels by evaluating force constants analytically. All of the computations were carried out using the Gaussian 09 program,[37] in which the fine grid (75, 302) is the default for evaluating integrals numerically.

The energetically low-lying $(C_4H_6)_2M$ species are shown in the figures. Each structure is designated as **M-nZ**, where **M** is the symbol of the central metal atom, **n** orders the structure according their relative energies predicted by the B3LYP* method, and **Z** designates the spin states, using **S**, **D**, **T**, **Q**, **P**, and **X** for the singlet, doublet, triplet, quartets, quintet and sextet states, respectively.

3. Results

The lower symmetry of acyclic olefins such as butadiene compared with cyclic unsaturated ligands, including cyclobutadiene, cyclopentadienyl, and benzene, leads to

different orientations of the two ligands in open sandwich compounds not possible for sandwich compounds derived from planar cyclic hydrocarbons such as the $(\eta^5\text{-}C_5H_5)_2M$ metallocenes. The ligand orientations in bis(butadiene)metal complexes $(\eta^4\text{-}C_4H_6)_2M$ can be characterized by the rotation angle of one tetrahapto butadiene ligand relative to the other similar butadiene ligand, designated as χ (Figure 4).[3] A meaningful value of the single parameter χ to define such conformations assumes that both butadiene ligands are planar or nearly planar. In order to describe χ, we define two vectors for the two $\eta^4\text{-}C_4H_6$ ligands. For each $\eta^4\text{-}C_4H_6$ ligand, this vector starts from the midpoint of the center C–C bond and goes toward the midpoint of the two terminal carbon atoms. We define χ as the angle between the two vectors for each $\eta^4\text{-}C_4H_6$ ligand. Thus the angle χ is taken as 0° if the $\eta^4\text{-}C_4H_6$ ligands have a *syn*-eclipsed orientation and 180° if the C_4H_6 ligands have an *anti*-eclipsed orientation (Figure 3). A χ angle of 90° corresponds to a staggered orientation of the two butadiene ligands.

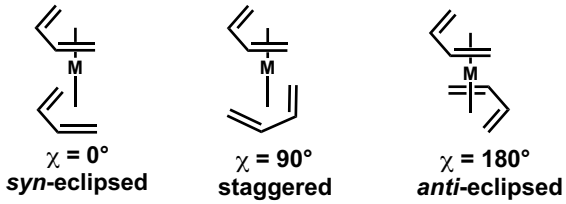

Figure 4. Definition of the rotation angle χ to describe the ligand conformations in bis(butadiene)metal $(\eta^4\text{-}C_4H_6)_2M$ open sandwich compounds.

The lowest energy $(C_4H_6)_2M$ structures all have a staggered conformation of the butadiene ligands corresponding to tetrahedral metal coordination. Considering the distribution of the d electrons in a tetrahedral field for the lowest energy $(\eta^4\text{-}C_4H_6)_2M$ structures is seen to rationalize perfectly their preferred spin states (Figure 5). Thus the spin states increase stepwise in the $(\eta^4\text{-}C_4H_6)_2M$ structures upon removing electrons from the filled d shell in singlet $(C_4H_6)_2Ni$ to give the three holes in the d shell in quartet $(C_4H_6)_2Mn$. Similarly, the spin states increase stepwise upon adding electrons to singlet $(C_4H_6)_2Ti$ to give quartet $(C_4H_6)_2Mn$.

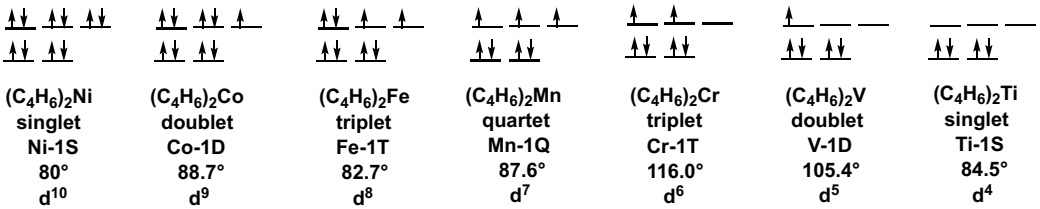

Figure 5. The configurations of the d electrons in the $(C_4H_6)_2M$ (M = Ti to Ni) derivatives in a tetrahedral ligand field.

3.1.1. $(C_4H_6)_2Ni$.

Only one low-energy $(C_4H_6)_2Ni$ structure was found, namely the C_2 singlet structure **Ni-1S** (Figure 6 and Table 1), with the two open chain butadiene ligands in a nearly staggered orientation (χ = 80°). In this structure, the Ni-C distances clearly indicate two tetrahapto η^4-C_4H_6 ligands, with the Ni-C distances shown in Figure 5. Thus, the nickel atom in **Ni-1S** has the favored 18-electron configuration.

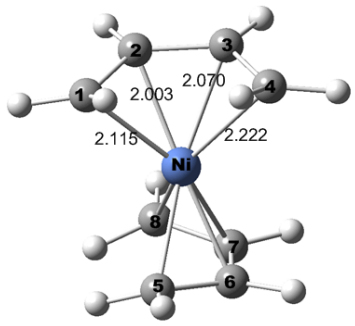

Ni-1S (C_2)

Figure 6. The optimized staggered $(C_4H_6)_2Ni$ structure. Distances are shown in Å.

Among the 18 valence electrons, ten originate from the 3d orbitals of the d^{10} nickel(0) atom (Figure 4), and other eight arise from the π bonds of the two butadiene ligandss. In other words, there are nine occupied MOs in $(C_4H_6)_2Ni$ composed of Ni d orbitals and C p orbitals. In order to provide some insight into the bonding of the butadiene ligands to the metal atom in the $(C_4H_6)_2Ni$ structure, its frontier molecular orbitals (MOs) were investigated including the four highest occupied orbitals and the two lowest virtual orbitals (Figure 7). All six of these frontier MOs show the nickel d atomic orbitals and the carbon p orbitals of the C_4H_6 ligands. Thus the HOMO and the other occupied orbitals (HOMO-1, HOMO-2, and HOMO-3), exhibit the bonding interaction between a nickel d orbital and butadiene carbon p orbitals. However, in the virtual (unoccupied) orbitals (LUMO and LUMO+1), the nickel d orbital and carbon p orbitals have opposite phases, indicating antibonding interactions between the metal atom and the C_4H_6 ligands.

3.1.6. $(C_4H_6)_2Co$.

Two low-energy doublet structures were found for the butadiene cobalt complex $(C_4H_6)_2Co$, namely the lowest-energy C_2 doublet structure **Co-1D** and the C_{2v} doublet structure **Co-2D**, lying 9.7 kcal/mol (B3LYP*) above **Co-1D** (Figure 8 and Table 2). The Co-C distances in **Co-1D** and **Co-2D** indicate that all of the butadiene units function as

tetrahapto ligands to the cobalt atom. In **Co-1D** the two η^4-C_4H_6 ligands have a staggered orientation (χ = 89°), while in **Co-2D** the two η^4-C_4H_6 ligands have a *syn*-eclipsed orientation (χ = 0°). In both **Co-1D** and **Co-2D** the cobalt atoms have a 17-electron configuration, consistent with their doublet spin states.

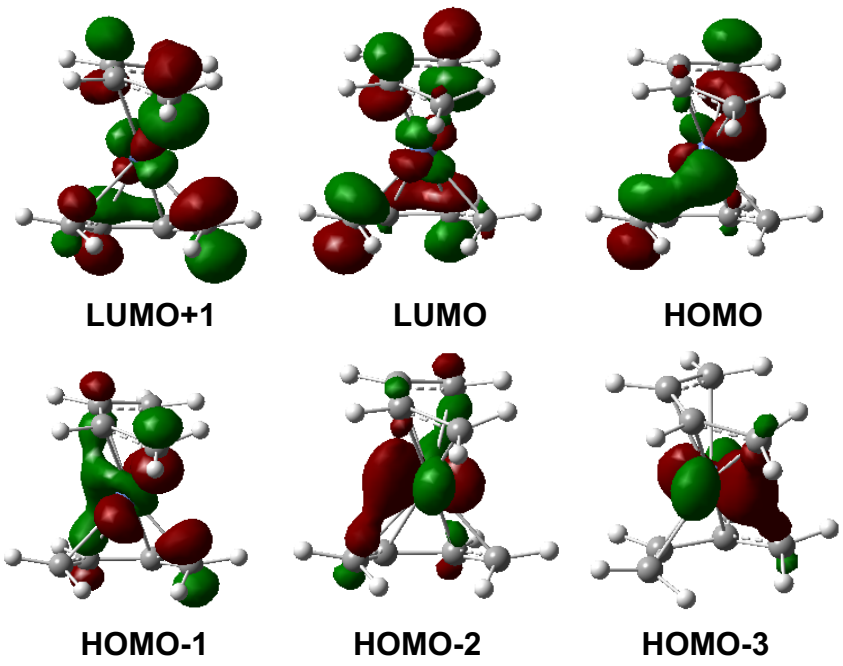

Figure 7. The frontier molecular orbitals of **Ni-1S**.

Table 1. Total energies (E, in hartree), total free energies (G, in hartree), HOMO and LUMO energies (in hartree), HOMO-LUMO gaps (in eV), butadiene ligand orientations, and the χ angles for the $(C_4H_6)_2Ni$ structures.

	Ni-1S (*C*$_2$)
E+1819	-1.03655
ΔE	0.0
G+1819	-0.89824
ΔG	0.0
Orientation	staggered
χ	80.4°
HOMO(α)	-0.18230
LUMO(α)	-0.04524
gap/eV	3.73

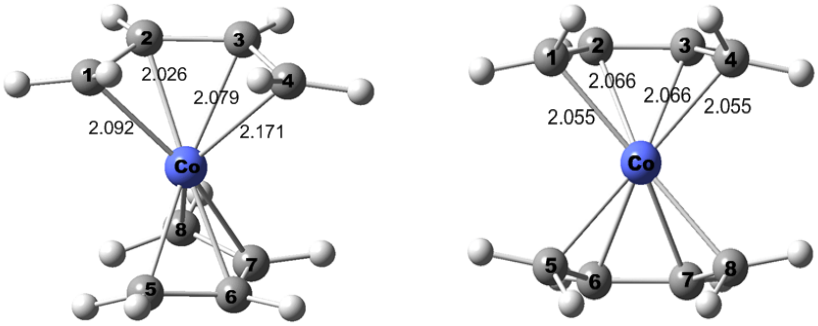

Figure 8. The optimized $(C_4H_6)_2Co$ structures. Distances are shown in Å.

Table 2. Total energies (E in hartree), total free energies (G, in hartree), relative energies (ΔE in kcal/mol), HOMO and LUMO energies (in hartree), HOMO-LUMO gaps (in eV), spin expectation values $\langle S^2 \rangle$, butadiene ligand orientations, and the χ angles for the $(C_4H_6)_2Co$ structures.

	Co-1D (C_2)	**Co-2D (C_{2v})**
E+1694	-0.49087	-0.47549
ΔE	0.0	9.7
G+1694	-0.35246	-0.33670
ΔG	0.0	9.9
Orientation	staggered	*syn*-eclipsed
χ	88.7°	0.0°
HOMO(α)	-0.19083	-0.15894
LUMO(α)	-0.04322	-0.04791
gap/eV	4.02	3.02
$\langle S^2 \rangle$	0.80	0.76

3.1.5. $(C_4H_6)_2Fe$.

Four low-energy $(C_4H_6)_2Fe$ structures (two triplets and two singlets) were found with butadiene ligands (Figure 9 and Table 3). The lowest-energy such structure predicted by B3LYP* is the C_1 triplet structure **Fe-1T**. The Fe-C distances in **Fe-1T** clearly indicate that the iron atom has two tetrahapto η^4-C_4H_6 ligands in a staggered conformation (χ = 88°). A C_2 triplet conformer **Fe-2T** lies 9.0 kcal/mol (B3LYP*) in energy above **Fe-1T**. The two tetrahapto η^4-C_4H_6 ligands in **Fe-2T** have a *syn*-eclipsed conformation (χ = 0°). The iron atoms in both **Fe-1T** and **Fe-2T** have 16-electron configurations corresponding to their triplet spin states.

The lowest energy singlet $(C_4H_6)_2Fe$ structures **Fe-1S** (C_2 symmetry) and **Fe-2S** (C_{2v} symmetry) are conformers, differing in the orientation of the two open chain butadiene ligands with χ = 103° for **Fe-1S** and χ = 0° for **Fe-2S** (Figure 9 and Table 3).

These two singlet structures lie 6.3 and 8.5 kcal/mol (B3LYP*), respectively, in energy above the lowest energy structure **Fe-1T**. The Fe-C distances suggest that all of the butadiene ligands are tetrahapto η^4-C_4H_6 ligands, thereby giving the iron atoms in **Fe-1S** and **Fe-2S** 16-electron configurations. Thus the singlet structures **Fe-1S** and **Fe-2S** appear to be low-spin isomers of the triplet structures **Fe-1T** and **Fe-2T**, respectively. Note that for the staggered ligand orientation with $\chi \approx 90^\circ$ the triplet structure **Fe-1T** has a distinctly lower energy than the corresponding singlet structure **Fe-1S**. However, for the *syn*-eclipsed ligand orientation with $\chi = 0$ the triplet structure **Fe-2T** and the corresponding singlet structure **Fe-2S** have essentially the same energies within ~0.4 kcal/mol.

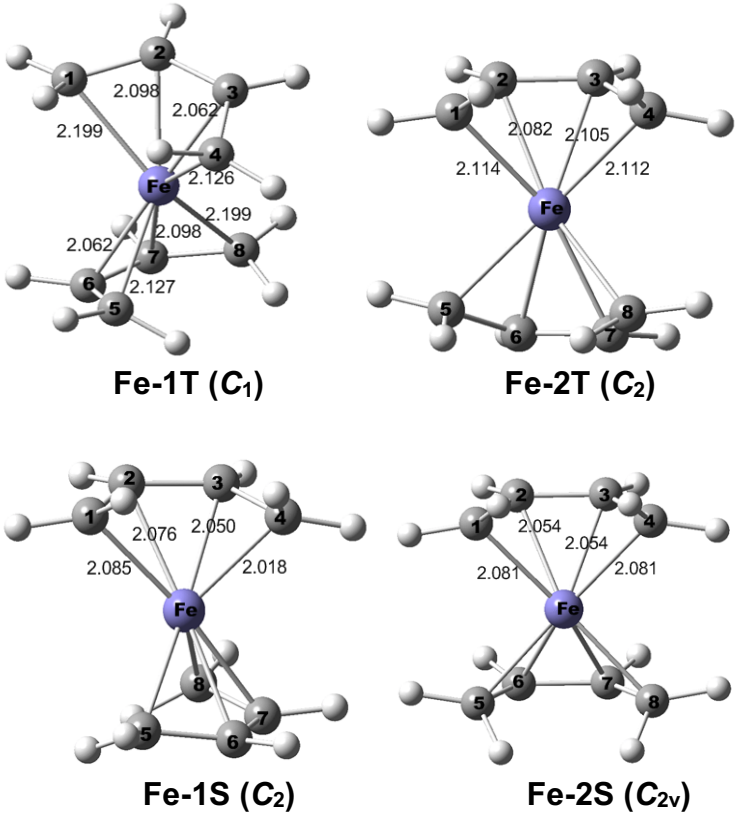

Figure 9. The optimized $(C_4H_6)_2Fe$ structures. Distances are shown in Å.

3.1.4. $(C_4H_6)_2Mn$.

Five low-energy structures with butadiene C_4H_6 ligands were optimized for $(C_4H_6)_2Mn$ (Figure 10 and Table 4). The lowest-energy structure predicted by the B3LYP* method is the C_2 quartet structure **Mn-1Q** with the two butadiene ligands in a staggered orientation with $\chi = 87.6°$ (Table 4). The Mn-C distances in **Mn-1Q** indicate that all eight carbon atoms in the two butadiene ligands are bonded to the manganese

atom, thereby giving the manganese atom a 15-electron configuration consistent with a quartet spin state.

Table 3. Total energies (E in hartree), total free energies (G, in hartree), relative energies (ΔE in kcal/mol), HOMO and LUMO energies (in hartree), HOMO-LUMO gaps (in eV), spin expectation values $\langle S^2 \rangle$, butadiene ligand orientations, and the χ angles for the $(C_4H_6)_2Fe$ structures.

	Fe-1T (C_1)	**Fe-2T (C_2)**	**Fe-1S (C_2)**	**Fe-2S (C_{2v})**
E+1575	-0.42419	-0.40997	-0.41421	-0.41063
ΔE	0.0	9.0	6.3	8.5
G+1575	-0.28825	-0.27306	-0.27410	-0.27013
ΔG	0.0	9.5	8.9	11.4
Orientation	staggered	eclipsed	staggered	eclipsed
χ	82.7°	20.3°	102.8°	0.0°
HOMO(α)	-0.19737	-0.15710	-0.18477	-0.19113
LUMO(α)	-0.04550	-0.05111	-0.07378	-0.08190
gap/eV	4.13	2.88	3.02	2.97
$\langle S^2 \rangle$	2.18	2.17	0.0	0.0

.

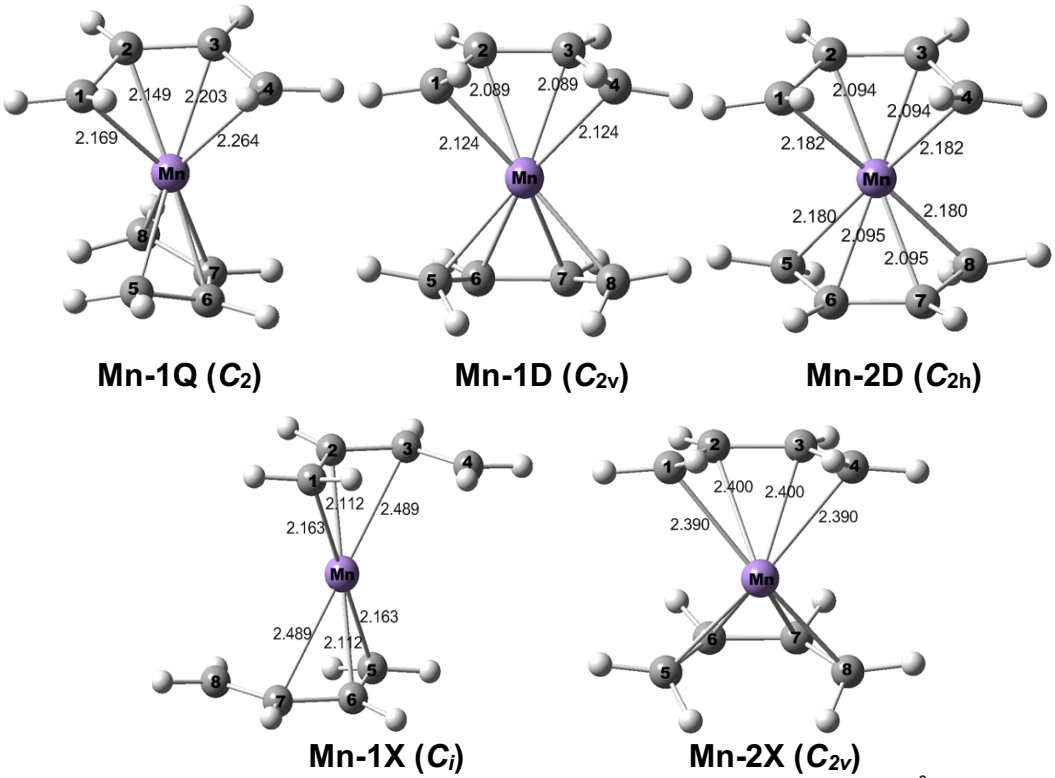

Figure 10. The optimized $(C_4H_6)_2Mn$ structures. Distances are shown in Å.

Table 4. Total energies (E in hartree), total free energies (G, in hartree), relative energies (ΔE in kcal/mol), HOMO and LUMO energies (in hartree), HOMO-LUMO gaps (in eV), spin expectation values $\langle S^2 \rangle$, butadiene ligand orientations, and the χ angles for the $(C_4H_6)_2Mn$ structures.

	Mn-1Q (C_2)	**Mn-1D (C_{2v})**	**Mn-2D (C_s)**	**Mn-1X (C_i)**	**Mn-2X (C_{2v})**
E+1462	-0.71245	-0.68943	-0.68058	-0.67913	-0.67318
ΔE	0.0	14.4	20.0	20.9	24.6
G+1462	-0.57837	-0.55200	-0.54680	-0.55056	-0.54432
ΔG	0.0	16.5	19.8	17.5	21.4
Orientation	staggered	eclipsed	eclipsed	eclipsed	eclipsed
χ	87.6°	0.0°	180.0°	180.0°	0.0°
HOMO(α)	-0.18833	-0.20222	-0.20969	0.13922	-0.14554
LUMO(α)	-0.05145	-0.08901	-0.09929	0.04585	-0.06727
gap/eV	3.72	3.08	3.00	2.54	2.13
$\langle S^2 \rangle$	4.08	1.02	1.89	8.83	8.79

Two doublet conformers **Mn-1D** (C_{2v} symmetry) and **Mn-2D** (C_{2h} symmetry) lie 14.4 and 20.0 kcal/mol (B3LYP*), respectively, above **Mn-1Q** (Figure 10 and Table 4). Structure **Mn-1D** has two open chain butadiene ligands in a *syn*-eclipsed orientation with θ = 0° (Table 4), while structure **Mn-2D** has two open chain butadiene ligands in an *anti*-eclipsed orientation with χ = 180° (Table 4). The Mn-C distances in both **Mn-1D** and **Mn-2D** suggest exclusively tetrahapto η^4-C_4H_6 ligands to give the manganese atoms 15-electron configurations.

Two sextet $(C_4H_6)_2Mn$ structures, namely the C_i structure **Mn-1X** and the C_{2v} structure **Mn-2X**, lie at higher energies of 20.9 and 24.6 kcal/mol (B3LYP*), respectively, above **Mn-1Q** (Figure 10 and Table 4). The Mn-C distances in **Mn-1X** and χ = 180° (Table 4) suggest two trihapto η^3-C_4H_6 ligands in a *anti*-eclipsed orientation, thereby giving the manganese atom a 13-electron configuration. The Mn-C distances in **Mn-2X** and χ = 0° (Table 4) indicate two tetrahapto η^4-C_4H_6 ligands in a *syn*-eclipsed orientation, giving the manganese atom a 15-electron configuration.

3.1.3. $(C_4H_6)_2Cr$.

Six low-energy $(C_4H_6)_2Cr$ structures were found with butadiene ligands, namely two singlet structures **Cr-1S** and **Cr-2S**, two triplet structures **Cr-1T** and **Cr-2T**, and two quintet structures **Cr-1P** and **Cr-2P** (Figure 11 and Table 5). The B3LYP* method

predicts the C_2 triplet **Cr-1T** to be the lowest energy structure. In **Cr-1T**, the dihedral angle (χ) of 116° shows a nearly staggered orientation of the two C_4H_6 ligands (Table 5). The other triplet $(C_4H_6)_2Cr$ structure **Cr-2T**, lying 5.3 kcal/mol in energy above **Cr-1T**, is found to be a C_2 symmetry conformer of **Cr-1T** with the two C_4H_6 ligands in a nearly *syn*-eclipsed orientation with χ = 12°. The Cr-C distances clearly indicate that the chromium atoms in **Cr-1T** and **Cr-2T** each have two tetrahapto η^4-C_4H_6 ligands, thereby giving each chromium atom a 14-electron configuration.

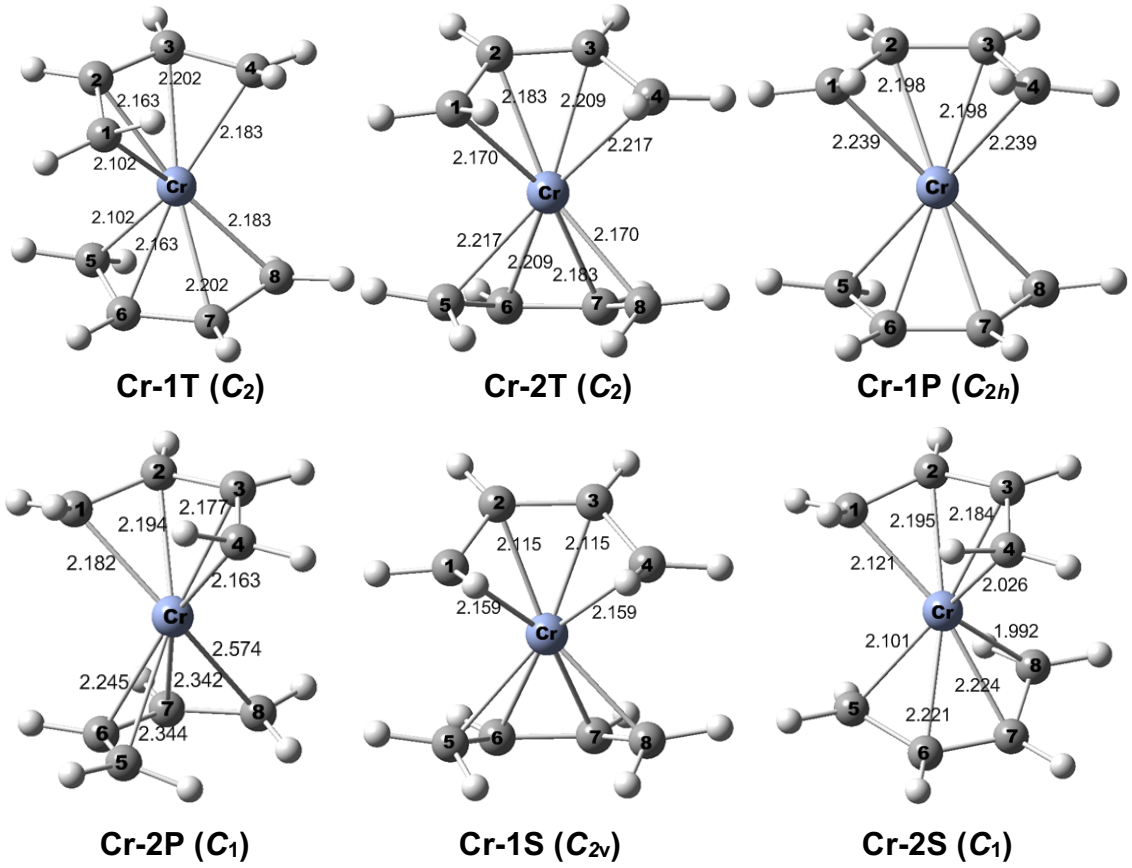

Figure 11. The optimized $C_8H_{12}Cr$ structures. The distances are in Å.

Two quintet $(C_4H_6)_2Cr$ structures **Cr-1P** (C_{2h} symmetry) and **Cr-2P** (C_1 symmetry), lying 9.6 and 12.0 kcal/mol in energy above **Cr-1T**, differ only by the orientation of the two tetrahapto η^4-C_4H_6 ligands (Figure 11). Structure **Cr-1P** has an *anti*-eclipsed orientation of the butadiene ligands with χ = 180°, whereas the χ value of 74.9° indicates a nearly staggered orientation of the butadiene ligands in **Cr-2P.** The Cr–C distances indicate tetrahapto coordination of both butadiene ligands in both **Cr-1P** and **Cr-2P** corresponding to 14-electron configurations for the chromium atoms.

Table 5. Total energies (E in hartree), total free energies (G, in hartree), relative energies (ΔE in kcal/mol), HOMO and LUMO energies (in hartree), HOMO-LUMO gaps (in eV), the spin expectation values $\langle S^2 \rangle$, butadiene ligand orientations, and the χ angles for the $(C_4H_6)_2Cr$ structures.

	Cr-1T (C_2)	**Cr-2T (C_2)**	**Cr-1P (C_{2h})**	**Cr-2P (C_1)**	**Cr-1S (C_{2v})**	**Cr-2S (C_1)**
E+1356	-0.18934	-0.18093	-0.17408	-0.17022	-0.15373	-0.14341
ΔE	0.0	5.3	9.6	12.0	22.3	28.8
G+1356	-0.05424	-0.04701	-0.04043	-0.03809	-0.01439	-0.00722
ΔG	0.0	4.5	8.7	10.1	25.0	29.5
Orientation	staggered	eclipsed	eclipsed	staggered	eclipsed	staggered
χ	116.0°	12.1°	180.0°	74.9°	0.0°	109.0°
HOMO(α)	-0.19306	-0.19594	-0.14258	-0.16603	-0.17068	-0.15781
LUMO(α)	-0.07692	-0.08183	-0.02829	-0.03919	-0.07546	-0.07216
gap/eV	3.16	3.10	3.11	3.45	2.59	2.33
$\langle S^2 \rangle$	2.26	2.37	6.04	6.12	0.0	0.0

The singlet $(C_4H_6)_2Cr$ structures **Cr-1S** (C_{2v} symmetry) and **Cr-2S** (C_1 symmetry) are significantly higher energy structures than their triplet and quintet isomers, lying 22.3 and 28.8 kcal/mol, respectively, above **Cr-1T** (Figure 11). In **Cr-1S** the butadiene ligands have a *syn*-eclipsed orientation with χ = 0° whereas in **Cr-2S** the butadiene ligands have a nearly staggered orientation with χ = 109°. The Cr-C distances in **Cr-1S** and **Cr-2S** indicate all tetrahapto η^4-C_4H_6 ligands, thereby giving the chromium atoms 14-electron configurations.

3.1.2. $(C_4H_6)_2V$.

Four low-energy $(C_4H_6)_2V$ structures were found having butadiene C_4H_6 ligands, namely the doublet structures **V-1D** and **V-2D** and the quartet structures **V-1Q** and **V-2Q** (Figure 12 and Table 6). The global minimum by B3LYP***** is the C_2 doublet structure **V-1D**. The two C_4H_6 ligands in **V-1D** have an approximately staggered orientation as indicated by a χ value of 105.4°. The other doublet $(C_4H_6)_2V$ structure **V-2D**, lying 1.8 kcal/mol in energy above **V-1D** (B3LYP*), has C_{2v} symmetry and is a conformer of **V-1D** with the two η^4-C_4H_6 ligands in a *syn*-eclipsed orientation as indicated by a χ value of 0. The V-C distances in **V-1D** and **V-2D** clearly indicate two tetrahapto η^4-C_4H_6 ligands, thereby giving their vanadium atoms a 13-electron configuration.

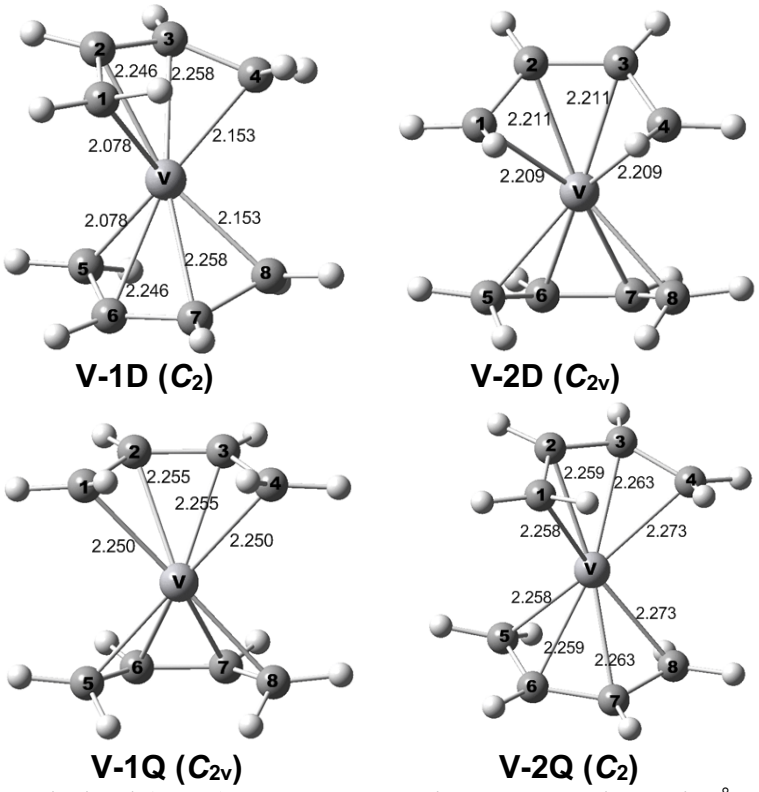

Figure 12. The optimized $(C_4H_6)_2V$ structures. Distances are shown in Å.

Table 6. Total energies (E in hartree), total free energies (G, in hartree), relative energies (ΔE in kcal/mol), HOMO and LUMO energies (in hartree), HOMO-LUMO gaps (in eV), the spin expectation values $\langle S^2 \rangle$, the butadiene ligand orientations, and the χ angles for the $(C_4H_6)_2V$ structures.

	V-1D (C_2)	**V-2D (C_{2v})**	**V-1Q (C_{2v})**	**V-2Q (C_2)**
E+1255	-0.71570	-0.71282	-0.70428	-0.70296
ΔE	0.0	1.8	7.2	8.0
G+1255	-0.58223	-0.57679	-0.57182	-0.57084
ΔG	0.0	3.4	6.5	7.1
Orientation	staggered	eclipsed	eclipsed	intermediate
χ	105.4°	0.0°	0.0°	131.2°
$\langle S^2 \rangle$	0.80	0.79	3.77	3.78
HOMO(α)	-0.18523	-0.18729	-0.16905	-0.16105
LUMO(α)	-0.08635	-0.07838	-0.05632	-0.06265
gap/eV	2.69	2.96	3.06	2.67

The two low energy quartet $(C_4H_6)_2V$ structures, namely the C_{2v} structure **V-1Q** lying 7.2 kcal/mol above **V-1T** and the C_2 structure **V-2Q** lying 8.0 kcal/mol above **V-1T**, are conformers (Figure 12 and Table 6). In **V-1Q** the η^4-C_4H_6 ligands have a

syn-eclipsed orientation as indicated by a χ value of 0°. However, in **V-2Q** the η^4-C_4H_6 ligands has a conformation between eclipsed and staggered as indicated by a χ value of 131°. The V–C distances in both **V-1Q** and **V-2Q** indicate exclusively tetrahapto η^4-C_4H_6 ligands thereby leading to 13-electron configurations for each vanadium atom.

3.1.1. $(C_4H_6)_2Ti$.

Only one low-energy $(C_4H_6)_2Ti$ structure was found containing butadiene ligands, namely the C_2 singlet structure **Ti-1S** (Figure 13 and Table 7). The dihedral angle χ of 84.5° shows a staggered orientation of the two η^4-C_4H_6 ligands. Our optimizations of possible other conformers of singlet bis(butadiene)titanium with χ as 0° or 180° do not lead to genuine minima., The Ti-C distances in **Ti-1S** clearly indicate tetrahapto η^4-C_4H_6 ligands thereby giving the titanium atom in **Ti-1S** a 12-electron configuration.

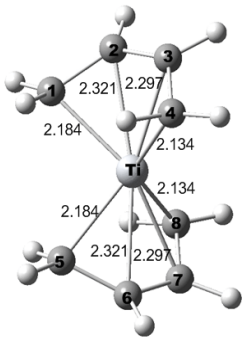

Ti-1S (C_2)

Figure 13. The $(C_4H_6)_2Ti$ structures optimized by the B3LYP* method.

Table 7. Total energies (E in hartree), total free energies (G, in hartree), HOMO and LUMO energies (in hartree), HOMO-LUMO gaps (in eV), and the χ angles for the $(C_4H_6)_2Ti$ structures.

	Ti-1S (C_2)
E+1161	-0.20171
ΔE	0.0
G+1161	-0.06803
ΔG	0.0
Orientation	staggered
χ	84.5°
HOMO(α)	-0.18138
LUMO(α)	-0.07201
gap/eV	2.98

These 12 valence electrons in **Ti-1S** are composed of four valence electrons from the d^4 titanium(0) atom (Figure 4) and eight valence electrons from the carbon p orbitals. Figure 14 shows the frontier molecular orbitals (MOs) for **Ti-1S**, including four occupied orbitals and four virtual orbitals. Similar to the structure **Ni-1S** the HOMO and other three occupied frontier orbitals down to HOMO–3 have the titanium d orbitals and the C_4H_6 carbon p orbitals in phase so they relate to bonding between the titanium atom and the C_4H_6 ligands. However, the LUMO and next three virtual orbitals up to LUMO+3 have the titanium d orbitals and the C_4H_6 carbon p orbitals out of phase so they relate to antibonding between the titanium atom and the C_4H_6 ligands.

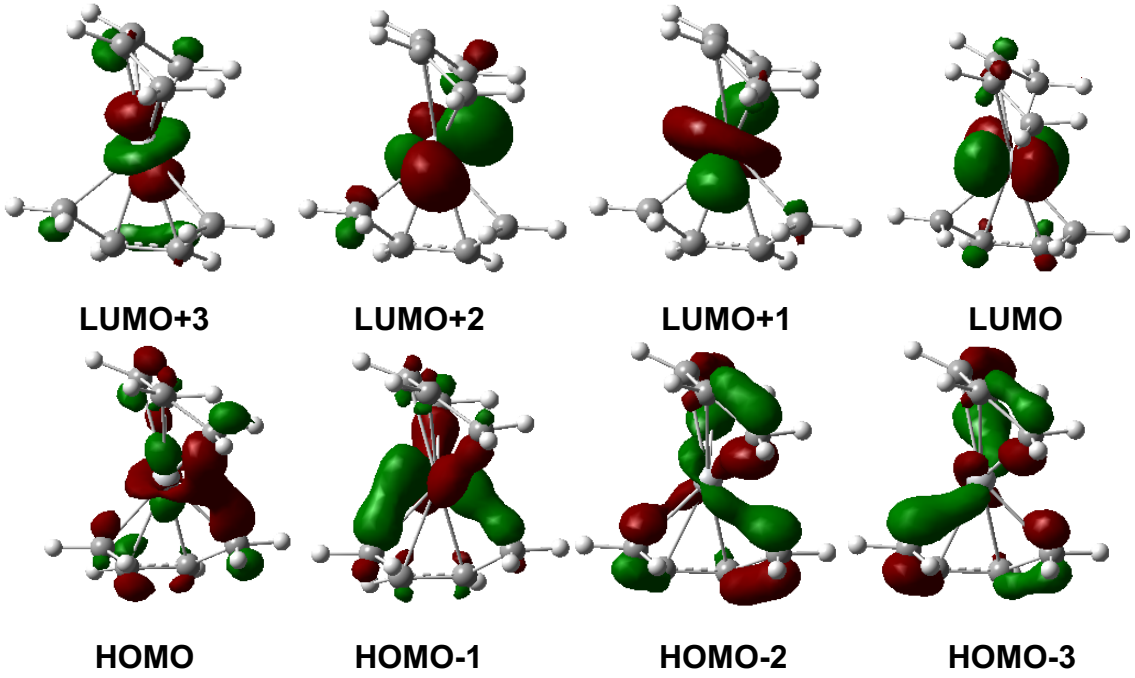

Figure 14. The frontier molecular orbitals of **Ti-1S**.

4. Discussion

In all of the $(C_4H_6)_2M$ structures discussed in this paper (except for the sextet $(C_4H_6)_2Mn$ structure **Mn-2X**) the butadiene units are tetrahapto ligands, as indicated by the M–C distances. However, tetrahapto butadiene ligands equivalently can be considered as small bite chelating bidentate diolefin ligands (Figure 15) so that the metal atoms in the $(\eta^4\text{-}C_4H_6)_2M$ complexes are formally tetracoordinate. Such bidentate diolefin coordination of butadiene to a single metal atom requires *cis* geometry of the butadiene ligand in order to have reasonable M–C bonding distances to all four butadiene carbon atoms.

The two fundamental types of metal coordination in tetracoordinate complexes are tetrahedral and square planar. Furthermore, the type of metal tetracoordination in bis(butadiene)metal complexes $(\eta^4\text{-}C_4H_6)_2M$ can relate to the rotation angle of the butadiene ligands χ if the butadiene ligand is considered as a small bite chelating diolefin (Figure 15). Thus staggered orientation of the two butadiene ligands in a $(\eta^4\text{-}C_4H_6)_2M$ derivative with an ideal χ value of 90° corresponds to tetrahedral coordination of the central metal atom. Similarly, an eclipsed orientation of both butadiene ligands with χ of 0° or 180, corresponds to a square planar coordination of the central metal atom.

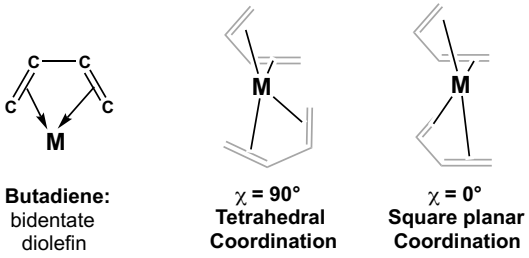

Figure 15. Butadiene as a bidentate chelating diolefin ligand.

The lowest energy $(C_4H_6)_2M$ structures all have a staggered conformation of the butadiene ligands corresponding to tetrahedral metal coordination. The deviation of the χ angle in these structures from the ideal χ = 90° varies from χ = 82.7° for the triplet $(C_4H_6)_2Fe$ structure **Fe-1T** to 116.0° for the likewise triplet $(C_4H_6)_2Cr$ structure **Cr-1T**. Considering the distribution of the d electrons in a tetrahedral field for the lowest energy $(\eta^4\text{-}C_4H_6)_2M$ structures is seen to rationalize perfectly their preferred spin states (Figure 5). Thus the spin states increase stepwise in the $(\eta^4\text{-}C_4H_6)_2M$ structures upon removing electrons from the filled d shell in singlet $(C_4H_6)_2Ni$ to give the three holes in the d shell in quartet $(C_4H_6)_2Mn$. Similarly, the spin states increase stepwise upon adding electrons to singlet $(C_4H_6)_2Ti$ to give quartet $(C_4H_6)_2Mn$.

5. Summary

The lowest energy bis(butadiene)metal structures $(C_4H_6)_2M$ (M = Ti to Ni) have a staggered orientation of the two butadiene ligands, corresponding to a tetrahedral coordination of the central metal atom to the four C=C double bonds of the butadiene ligands. Distribution of the metal d electrons in the resulting tetrahedral ligand field rationalizes the predicted spin states. These increase monotonically from singlet to quartet from nickel to manganese and back from quartet to singlet from manganese to titanium.

Conflicts of Interest. There are no conflicts of interest to declare.

Acknowledgments. This work is supported by the Chunhui Plan of the Chinese Educational Ministry (Grant No. Z2016159), the National Natural Science Foundation of China (Grant No. 11647058, 11605143), the key Project of Education Department of Sichuan Province (Grant No.17ZA0369), and the fund of the Key Laboratory of Advanced Scientific Computation, Xihua University, China. Research at the University of Georgia was supported by the U. S. National Science Foundation (Grant CHE-1661604).

Supporting Information. Tables S1 to S23: Atomic coordinates of the optimized structures for the $(C_4H_6)_2M$ (M = Ni, Ti, Co, Fe, Mn, Cr, V) complexes; Tables S24 to S46: Harmonic vibrational frequencies (in cm^{-1}) and infrared intensities (in parentheses in km/mol) for the $(C_4H_6)_2M$ (M = Ni, Ti, Co, Fe, Mn, Cr, V) complexes; Tables S47 to S53: The distances (in Å) of M-C bonds for the $(C_4H_6)_2M$ (M = Ni, Ti, Co, Fe, Mn, Cr, V) complexes; Tables S54 to S60: Total energies (E in hartree), relative energies (ΔE in kcal/mol), HOMO and LUMO energies (in hartree), HOMO-LUMO gaps (in eV), the spin expectation $\langle S^2 \rangle$ values, the χ angles for the $(C_4H_6)_2M$ (M = Ni, Ti, Co, Fe, Mn, Cr, V) complexes by all three methods; Complete Gaussian09 reference (Reference 37).

Literature References

(1) Kealy, T. J.; Pauson, P. L. *Nature* **1961**, *168*, 1039.
(2) Miller, S. A.; Tebboth, J. A.; Tremaine, T. F. *J. Chem. Soc.* **1952**, *3*, 632.
(3) Ernst, R. D. *Chem. Rev.* **1988**, *88*, 1255.
(4) Fischer E. O.; Hafner, W. *Z. Naturforsch.*, **1955**, *10b*, 665.
(5) Emerson, G. F.; Watts, L.; Pettit, R. *J. Am. Chem. Soc.* **1965**, *87*, 131.
(6) Hoberg, H.; Krause-Goeing, R.; Mynott, R. *Angew. Chem.* **1978**, *90*, 138.
(7) Hoberg, H.; Froelich, C. *J. Organometal. Chem.* **1979**, *168*, C52.
(8) Reihlen, O.; Gruhl, A.; Hessling, G.; Pfrengle, O. *Liebigs Ann. Chem*., **1930**, *482*, 161.
(9) Hallam, B. F.; Pauson, P. L. *J. Chem. Soc.,* **1958**, 642.
(10) Mills, O. S.; Robinson, G. *Acta. Cryst.,* **1963**, *16*, 758.
(11) Skell, P. S.; Havel, J. J.; Williams-Smith, D. L.; McGlinchey, M. J. *Chem. Commun.* **1972**, 1098.

(12) Cloke, F. G. N.; McCamley, A. *Chem. Commun.* **1991**, 1470.
(13) Cloke, F. G. N.; Hitchcock, P. B.; McCamley, A. *Chem. Commun*. **1993**, 248.
(14) Cloke, F. G. N.; Gardiner, M. G.; Raston, C. L.; Simpson, S. J. *J. Organometal. Chem.* **1996**, *507* 245.
(15) Koerner von Gustorf, E.; Buchkremer, J.; Pfajfer, Z.; Grevels, F. W. *Angew. Chem. Int. Ed.* **1971**, *10*, 260.
(16) McCall, J. M.; Morton, J. R.; Le Page, Y.; Preston, K. F. *Organometallics* **1984**, *3*, 1299.
(17) Herberhold, M.; Razavi, A. *Angew. Chem.* **1975**, *87*, 351.
(18) Herberhold, M.; Neugebauer, D.; Razavi, A. *Angew. Chem.* **1975**, *87*, 352.
(19) Harlow, R. L.; Krusic, P. J.; McKinney, R. J.; Wreford, S. S. *Organometallic*s **1982**, *1*, 1506.
(20) Ziegler T.; Autschbach, J. *Chem. Rev.* **2005**, *105*, 2695.
(21) Bühl, M.; Kabrede, H. *J. Chem. Theory Comput.* **2006**, *2*, 1282.
(22) Brynda, M.; Gagliardi, L.; Widmark, P. O.; Power, P. P.; Roos, B. O. *Angew. Chem. Int. Ed.* **2006**, *45*, 3804.
(23) Sieffert, N.; Bühl, M. *J. Am. Chem. Soc.* **2010**, *132*, 8056.
(24) Schyman, P.; Lai, W.; Chen, H.; Wang, Y.; Shaik, S. *J. Am. Chem. Soc.* **2011**, *133*, 7977.
(25) Adams, R. D.; Pearl, W. C.; Wong, Y. O.; Zhang, Q.; Hall, M. B.; Walensky, J. R. *J. Am. Chem. Soc.* **2011**, *133*, 12994.
(26) Lonsdale, R.; Olah, J.; Mulholland, A. J.; Harvey, J. N. *J. Am. Chem. Soc*. **2011**, *133*, 15464.
(27) Becke, A. D. *J. Chem. Phys*. **1993**, *98*, 5648.
(28) Lee, C.; Yang, W.; Parr, R. G. *Phys. Rev. B* **1988**, *37*, 785.
(29) Becke, A. D. *Phys. Rev. A* **1988**, *38*, 3098.
(30) Perdew, J. P. *Phys. Rev. B* **1986**, *33*, 8822.
(31) Reiher, M.; Salomon, O.; Hess, B. A. *Theor. Chem. Acc.* **2001**, *107*, 48.
(32) Salomon, O.; Reiher, M.; Hess, B. A. *J. Chem. Phys.* **2002**, *117*, 4729.
(33) Dunning, T. H. *J. Chem. Phys*. **1970**, *53*, 2823.
(34) Huzinaga, S. *J. Chem. Phys*. **1965**, *42*, 1293.
(35) Wachters A. J. H. *J. Chem. Phys*. **1970**, *52*, 1033.
(36) Hood, D. M.; Pitzer, R. M.; Schaefer, H. F. *J. Chem. Phys*. **1979**, *71*, 705.
(37) Frisch, M. J.; *et al.* Gaussian 09, Revision A.02; Gaussian, Inc., Wallingford CT, 2009.